Current Eye Research, 2019

Non-Orthogonal Refractive Lenses for Non-Orthogonal Astigmatic Eyes

Ahmed Abass[1*], Bernardo T Lopes[1, 2], Steve Jones[1], Lynn White[3],

John Clamp[3], Ahmed Elsheikh[1, 4, 5]

[1] School of Engineering, University of Liverpool, Liverpool, UK

[2] Department of Ophthalmology, The Federal University of São Paulo, São Paulo, Brazil

[3] Department of Research and Development, UltraVision CLPL, Leighton Buzzard, UK

[4] National Institute for Health Research (NIHR) Biomedical Research Centre at Moorfields Eye Hospital NHS Foundation Trust and UCL Institute of Ophthalmology, London, UK

[5] School of Biological Science and Biomedical Engineering, Beihang University, Beijing, China

[*] **Author for correspondence:**

Dr Ahmed Abass

School of Engineering, University of Liverpool, Liverpool, L69 3GH, UK.

A.Abass@liverpool.ac.uk

Keywords: cornea; astigmatism; non-orthogonal astigmatism; optical power; non-orthogonal lens

Number of words: 4449

Abstract

Purpose: To present a novel design method for non-orthogonal lenses to reduce the problem of residual astigmatism in non-orthogonal, astigmatic eyes

Methods: A method to create spectacle trial lenses with non-orthogonal power axes was developed based on a novel optimised light ray-tracing algorithm rather than conventional lens design methods which could not fully eliminate spherical aberration. Using this method, three sets of refraction trial lenses were made with the angles between power axes of each set controlled at 80°, 70° and 60°, respectively. Within each set, the cylindrical power varied from -1.00 D to -6.00 D in 1.00 D steps in addition to a -0.50 D lens. Computer-based numerical simulation of the lenses optical performance was carried out to apply orthogonal and non-orthogonal lenses on simulated astigmatic eyes. Subsequently, three clinical trial cases were investigated.

Results: Computer-simulated optical performance of non-orthogonal lenses showed the ability to achieve high performance in correcting non-orthogonal astigmatism. Subsequently, three patients with irregular astigmatism were refracted with the non-orthogonal lens sets, and clinically observed improvement at least two lines in the LogMAR chart was achieved in all three cases, compared with correction with orthogonal lenses, along with subjective improvement in image quality.

Conclusions: Non-orthogonal astigmatism, which is commonly ignored by current eye prescription systems, is taken into account in this study in the design of spectacle and soft contact lenses. The new approach considers the possible non-orthogonal positions of the eye's two optical power meridians and appears to be better able to correct the vision of irregular astigmatic eyes and significantly reduce residual astigmatism.

Introduction

It has been more than two centuries since astigmatism was first described (1, 2) and categorised as either orthogonal or non-orthogonal (3). While in orthogonal astigmatism, the flat and steep meridians are located at 90˚ to each other, the angle between the principal power meridians in non-orthogonal astigmatism varies from 90˚.

The existing system of prescribing a correction lens to a patient with an astigmatic eye consists of a combination of spherical and cylindrical lenses to form a single sphero-cylindrical lens (4). In this lens, the spherical component is responsible for correcting near or farsightedness and the cylindrical component is added to correct astigmatism. The current method of correcting the eye's refractive error is based on the assumption that the lowest and highest power meridians in an astigmatic visual system are always at a right angle to each other (Figure 1). However, if the power axes of a patient are not orthogonal, there will be residual astigmatism even if the best possible orthogonal refractive lenses are used to correct the patient's vision. Moreover, the software programs that control the operation of corneal topographers assume power axes are orthogonal in producing their power map outputs, making it impossible to assess the extent of non-orthogonal astigmatism present in individual eyes. Considering that up to 25% of the normal population have non-orthogonal astigmatism (3), it is important to revise the existing system of correcting astigmatism. This study addresses this need and presents a novel lens design method conceived to address the problem of residual astigmatism in non-orthogonal astigmatic eyes.

Materials and Methods

The lens design method and the patient case studies were approved by the Ethics Committee of the Federal University of São Paulo (Brazil) and conducted in accordance with the standards set out in the Declaration of Helsinki.

Lens design with non-orthogonal power axes

Unlike traditional prescription systems, the non-orthogonal lens design method relies on the maximum and minimum refractive powers P_1, P_2 and their corresponding angles A_1, A_2 in the form [P_1@A_1 & P_2@A_2]. The

back-surface of the lens is first designed according to the type of lens; whether it is a spectacle lens or a contact lens. While the back-surface of a spectacle lens is optimised to achieve a thickness t that would minimise the material needed to manufacture the lens and consequently, its weight, the back-surface of a contact lens is designed to enable comfortable fitting on the eye. The front-surface is then designed such that the combined power of the front and back surfaces of the lens, P_f and P_b, at a certain meridian should equal the total power, P , required at this meridian:

$$P = P_f + P_b \qquad (1)$$

This meant that the total surface power at this meridian P could be a combination of many different values of P_f and P_b, Figure 3. Controlling the back-surface design was always possible, either for spectacles or contact lenses, with no effect on the overall lens power as the front-surface of the lens was designed to adjust the overall lens power and to compensate for any specific shape of the back-surface. As a lens optical power can be described by its ability to refract the light, the total lens's refraction power is the result of the discrete refraction power of the front-surface and the back-surface of the lens. As a result, designing a lens that has a certain total optical power could be achieved through an infinite number of compensations between the geometry of the front-surface and the back-surface of the lens with the same material. This fact gives the designer the scope needed to put on some restrictions on one surface, then determine the other surface in a way that keeps the lens's total power as desired. Figure 3 shows eight possible designs as an example of a lens with a power of $P = -10$ dioptre where the front-surface and the back-surface powers P_f and P_{fb} were varying.

The design method is based on the fact that a surface with a certain power P would refract parallel light rays to a focal length $l = \frac{n}{P}$ where n is the refractive index of the medium beyond the surface. This process was carried out over the lens meridians one after another by tracing light rays following Snell's law (5). Each meridian was constructed by a series of nodes that were equally spaced along the meridian length. At these nodes, the optical powers of the Back-surface were $P_{b1}, P_{b2}, \dots, \dots$ (Figure 4) and the corresponding focal lengths were $l_{b1}, l_{b2}, \dots, \dots$, respectively (Figure 5Aa). The design is then completed by moving the corresponding meridian nodes on the front-surface outwards until the focal lengths at all nodes were equal to the desired focal length $l_f = \frac{n_{air}}{P}$ (Figure 5Ab). An optimisation process was then carried out to reposition the front meridian nodes in the anterior-posterior direction such that most of the refracted light rays fall on the

desired focal point. In case the designer needed to create the back-surface of the lens by setting its radius of curvature r, the equivalent optical power to r was determined as Equation 2.

$$P_b = \frac{n_{air} - n_{lens}}{r} \quad (2)$$

after which the optimisation process was carried out. After solving the back-surface optimisation process, the optical power of this surface was determined.

1. Front-surface design

In order to design the front-surface for the same lens, the front-surface power had to be calculated first as Equation 3

to $$P_f = P - P_b \quad (3)$$

ensure that the required overall lens power would be achieved. At that point, all optical powers at the front-surface nodes $P_{f1}, P_{f2}, \dots, P_{f6}$ had to be adjusted to be equal to P_f by altering the position of meridian nodes to satisfy the equation, Figure 5B,

$$l_{f1}, l_{f2}, \dots, l_{f6} = l_f = \frac{n_{lens}}{P_f} \quad (4)$$

where $l_{f1}, l_{f2}, \dots, l_{f6}$ are the focal lengths of the front-surface meridian nodes (Equation 4).

The presented non-orthogonal lens design process was based on the light ray-tracing method as can be seen in the flow chart in Figure 2. Initially, clinical data were collected to identify the patient's best non-orthogonal prescription.

Non-orthogonal simulated corneas

The overall purpose of simulating the new lens designs was to numerically quantify the issues with the conventional orthogonal lens design and to assess the need for a new design. Therefore, two idealised corneal surface models, with a significant difference in astigmatism, were constructed to enable studying the optical performance of the human eye using an optical light ray-tracing technique. While the first cornea model had orthogonal astigmatism of -5.0 dioptre (D) at 90°, the second model had non-orthogonal

astigmatism of -5.0 D at 45°. Both models needed no refractive correction along their nasal-temporal line at 180°. The visual performance of two hypothetical astigmatic corneas was simulated with the central corneal thickness being set to the average normal range of 0.545 mm. Both corneas had 43.050 D curvature on the flattest meridian and 48.053 D on the steepest meridian. The power of the back-surface of both corneas was set to -5.882 D, however, the front-surface power was set to 48.935 D at the flattest meridian and 53.935 D at the steepest meridian.

Clinical validation

In order to validate clinically the non-orthogonal design method, three sets of spectacle trial lenses with non-orthogonal power axes were manufactured and tested on subjects with irregular astigmatism. Commercial trial sets for eye examinations require over 200 individual pieces. As it was impracticable to manufacture this number of non-orthogonal lenses in the first instance, lens powers and non-orthogonal axes were targeted towards the prescriptions of the subjects. The power axes of each set were oriented such that the internal angles between the axes were 80°, 70° and 60°, respectively. In addition, a fourth set with orthogonal power axes was manufactured to act as a control set in the study. Each of the four sets included lenses with cylindrical powers of -1.00 DC to -6.00 DC in 1.00 DC steps (in addition to one -0.50 DC lens for fine adjustments). This range gave the potential prescription sensitivity of 0.50 DC steps, as subjects with aberrated corneas tend to be insensitive to 0.2 DC steps in spectacle refraction. However, 0.25 DS lenses were available from a conventional trial lens set to optimise spherical correction. These non-orthogonal cylinder sets were tested on three subjects with irregular astigmatism including two with mild keratoconus and one with longstanding, non-strabismus amblyopia. The refraction in each case was assessed using a standard LogMAR chart. The chart was changed randomly while testing lenses from the four sets.

For each subject, the refraction starting point was taken from the orthogonal spectacle prescription and the visual acuity recorded, as well as a subjective assessment of the visual quality. There is currently no methodology in the literature aimed at non-orthogonal refraction and it is unknown how valid the visual tools available to assist in refraction of orthogonal astigmatism would be in refracting with non-orthogonal lenses. Thus, the refractive technique was kept as basic and as familiar to the subject as possible to avoid introducing unknown variables. In refracting subjects with irregular corneas, often the best way of establishing the optimal axis is to allow the subject to rotate the lens in the trial frame. Subjects will subjectively balance optimal

contrast with minimal “ghosting” and “shadowing”. This method was used to attain the original orthogonal prescription, together with the use of spheres and cylinders lenses.

The subjects were then initially presented with a non-orthogonal cylinder of the same value as their orthogonal prescription from each set of lenses and were asked to locate the point of optimal acuity by rotating the lens to find the best axis position. This process was independently checked by the examiner by rotating the lens off-axis either way and asking the subject to indicate the optimal position. In order to ensure that the subject was not experiencing a placebo effect, the lenses were randomly “flipped” during the examination. Unlike conventional cylinder lenses, which present the same power meridians whichever way the lens is presented to the eye, non-orthogonal lenses present meridians at different axes when flipped which should cause an obvious difference in visual acuity. In all cases, the subjects were very clear that the “flipped” lens gave significantly worse visual acuity.

Topography data collection

Topography data for the subjects, relating to the geometrical characteristics of eyes, were exported from an Eye Surface Profiler ® (ESP, Eaglet Eye b.v., the Netherlands). Raw height data for the anterior surfaces were exported and analysed using a custom-built MATLAB® code (MathWorks, Natick, USA). Optical power maps based on corneal axial curvature were created using the collected height data and processed by MATLAB to detect the natural maximum and minimum corneal power meridians. Eye topography scans were carried out in a darkened room as light falling on the topographer during the scan may affect the measurement. As the topographer being used must be attached to a computer, the computer monitor was positioned to direct its light away of the participant’s face and set to a low brightness level. Participants were requested not to wear their soft contact lenses for at least two weeks before the topography measurement.

Results

Non-orthogonal refraction simulation

The geometry of the simulated corneal model was built by optimising the corneal front-surface through the light ray-tracing method with -5.00 D astigmatism at 90° for the first cornea which produced an orthogonal simulated corneal keratometry (Sim-K) of 43.05 D at 180° and 48.19 D at 90° (Figure 6a). However, the geometry of the second simulated corneal model was built with non-orthogonal astigmatism of -5.00 D at 45° (Figure 6b), which produced a Sim-K of 43.4 D at 158° and 47.85 D at 67.5° in the orthogonal meridians. The first cornea could be corrected by a toric spectacle lens with a power of -5.00 D at 90° (Figure 6b). However, to correct the equivalent orthogonal power of the second cornea, a different toric spectacle lens with a power of -0.35 D at 158° and -4.8 D at 67.5°, was required (Figure 6e). As can be seen from Figures 6c and f, orthogonal spectacle lens design was only able to correct the orthogonal astigmatic cornea (Figure 7c). Correcting the refractive error of a non-orthogonal cornea by a conventional orthogonal toric spectacle lens leaves residual astigmatism (Figure 6f). When the corneal non-orthogonality was taken into account by designing a non-orthogonal spectacle lens (Figure 6g), a stable refractive correction was possible as shown in Figure 6h.

Clinical validation

As the refraction simulation process demonstrated the expected benefits of the new designed non-orthogonal spectacle lenses, the study was developed to investigate the benefits of these spectacle lenses clinically. The clinical validation process was carried out in three case studies:

Case A: A 52-year-old male with mild keratoconus in the left eye, Figure 7A. His best spectacle lens prescription was -0.75 DS -2.25 DC @ 90°, with which his visual acuity was 6/9 but accompanied by significant ghosting, shadowing and visual disturbance. Slit lamp and retinal evaluation were unremarkable. Intraocular pressure (IOP) was 18 mmHg.

It was found that after refracting with non-orthogonal trial spectacle lenses, a non-orthogonal prescription of -1.75 D @ 80° / -2.50 D @ 140° (i.e. power meridians were 60° apart rather than being orthogonal) gave

visual acuity of 6/4. The ghosting and visual disturbances were significantly decreased. In fact, the subject reported that the visual experience was more aligned with his non-keratoconic eye.

Case B: A 47-year-old male with mild to moderate keratoconus in the left eye, Figure 7B. In this case, the distortion arising from keratoconus was inferior, not directly on the line of sight. His best-corrected spectacle prescription was OS Plano/-2.50 D @ 95 VA 6/5 but this was marred by extensive ghosting and visual distortion (most people suffering from keratoconus tend to be good at interpreting blurred images). IOP was 17 mmHg.

The subject was refracted with a non-orthogonal lens of prescription Plano @ 85° / -2.50 D @ 15°, with the two power meridians at 70° from each other rather than 90° (orthogonal). The subject found that with this non-orthogonal lens he could easily attain the 6/4 line on the LogMar chart and noted significant improvement in visual quality with almost total elimination of subjective ghosting effects.

Case C: A 49-year-old female with a long-term history of reduced visual acuity in the right eye, assumed to be refractive amblyopia, Figure 7C. Her clinical ophthalmic exam, including slit lamp, retinal and IOP measurements, were unremarkable. The best spectacle refraction was OD +3.75 DS -2.75 DC x 90° with VA 6/24 and OS +1.75 DS -0.75 DC @ 80° with VA 6/6, respectively. IOP was 19 mmHg.

Although amblyopic, analysis of her cornea showed she also suffered from irregular astigmatism which had never been corrected properly with regular toric spectacle lenses. Refraction using non-orthogonal lens trial lenses gave a non-orthogonal prescription of OD +4.00 D @ 10°/-3.25 D @ 130°, with which she attained 6/7.5. Assessment of her depth perception using the TNO test showed she could attain 60 seconds arc stereopsis. With normal spectacle correction, she could not attain any stereopsis using the TNO test.

Discussion

The prevalence of clinically significant astigmatism with more than 0.75 DC exceeds 30% of the world's population (6-10). Uncorrected astigmatism has several implications on the patient's life. It reduces significantly the safety in driving and affects reading fluency (16, 17). It is more prevalent among patients who suffer from migraine headaches and is positively correlated with the duration of a migraine attack (18, 19).

The assumption of orthogonality between steep and flat meridians in corneal power maps is a common feature in both the analysis of astigmatism and clinical practice to determine the eye's visual acuity, even though the possibility of meridional power non-orthogonality has been identified previously and is present in around 30% of astigmatic eyes (3, 11-15).

The difficulty of treating non-orthogonal optical power with refractive lenses is acknowledged in the literature and can be a contributing factor to higher order aberrations, which could not be corrected by toric refractive lenses (12, 20). These sphero-cylindrical lenses can leave uncorrected residual astigmatism in cases where the power axes are not orthogonally oriented.

Correcting higher order aberrations is complex, although it can be achieved with the use of rigid contact lenses or refractive surgery (21, 22). However, rigid contact lenses can only correct anterior corneal astigmatism, which is usually compensated by opposite internal astigmatism (23). Therefore, in cases where the corneal and the internal astigmatism axes are in opposite directions, wearing a rigid contact lens may produce a reduction in overall visual acuity. In many cases, where non-orthogonal astigmatism is present, the use of a non-orthogonal spectacle correction or non-orthogonal toric soft contact lens, can provide good visual acuity. In this context, an enquiry like 'where does non-orthogonal astigmatic optics end and high order aberrations begin?' is an interesting query to discuss. The Zernike polynomials are sets of polynomials function of two variables, radius (r) and angular position (θ) that are orthogonal inside the unit circle (24,25). Therefore, Zernike polynomials mask non-orthogonal astigmatism due to their reliance on orthogonal functions. As a result, non-orthogonal astigmatism cannot be quantified distinctly by Zernike polynomials as it is usually included among high order aberration terms. Consequently, there is no hard border between non-orthogonal astigmatism and Zernike's high order aberrations as the human eye geometry has a degree of non-orthogonality (3) even if its surface could be approximated to the summation of terms of orthogonal functions like Zernike polynomials.

As the presented method was developed for designing a lens for optimal optic performance, the design process considered only the 4 mm diameter central optical zone of the lens, and for this reason, the design of the peripheral zone should be considered separately. It was thus not possible to assess the peripheral effects of correcting with non-orthogonal spectacle lenses in a full spectacle frame and thus requires further study.

The original intent of this study was to show that visual acuity could be improved by the application of a non-orthogonal correction and this was clearly shown in the three cases presented. In normal clinical practice, the improvement of visual acuity in irregular cornea subjects is attained by regularising non-orthogonal astigmatism, usually by contact lens correction. Subsequent refraction optimisation can then be carried out in the normal way. With non-orthogonal refraction, a new methodology will be required. However, the further development of a refractive routine and the associated visual tools for correcting non-orthogonal astigmatism are beyond the scope of this study.

In conclusion, this study presented a new lens design method that offers an effective, non-invasive and cost-effective approach for correcting non-orthogonal astigmatism. Production of non-orthogonal lenses may not cause significant cost increases as the computer numerically controlled (CNC) machines commonly used in making lenses can be adjusted easily to introduce non-orthogonality. However, the new design method makes it necessary to use a significantly larger lens trial set, which both add to the cost of the set and the fitting time, but this may be necessary to enable the effective correction of non-orthogonal astigmatism.

Declaration of interest

All authors of this article declare no conflict of interest.

Acknowledgements

This work was funded by Innovate UK Knowledge Transfer Partnership Programme Grant No. 009521/UVP016.

List of figures

Figure 1: Forming a lens consists of spherical and cylindrical refractive bodies

Figure 2: Lens design flow chart

Figure 3: Eight different designs for a lens with a power of -10.0D. The refractive index of the lens material was 1.44 and its central thickness was 0.25mm

Figure 4: Designed meridian constructed from nodes

Figure 5: (A) Lens Back-surface design process, (B) Lens Front-surface design process

Figure 6: Theoretical justification of using a non-orthogonal lens design

Figure 7: Refractive power maps for participants

References

1. Atchison DA, Charman WN. Thomas Young's contribution to visual optics: the Bakerian Lecture "on the mechanism of the eye". J Vis. 2010;10(12):16.

2. Henderson BA, Gills JP. A Complete Surgical Guide for Correcting Astigmatism: An Ophthalmic Manifesto. Thorofare, USA: SLACK; 2011.

3. Abass A, Clamp J, Bao F, Ambrosio R, Jr., Elsheikh A. Non-Orthogonal Corneal Astigmatism among Normal and Keratoconic Brazilian and Chinese populations. Curr Eye Res. 2018; 43(6):717-724.

4. Jalie M. The principles of ophthalmic lenses. 5 ed. London, England: Association of Dispensing Opticians; 1972. 478 p.

5. Sabra AI. Theories of Light: From Descartes to Newton, UK: Cambridge University Press; 1981.

6. Schellini SA, Durkin SR, Hoyama E, Hirai F, Cordeiro R, Casson RJ, Selva D, Padovani CR. Prevalence of Refractive Errors in a Brazilian Population: The Botucatu Eye Study. Ophthalmic Epidemiology. 2009;16(2):90-7.

7. Liang YB, Wong TY, Sun LP, Tao QS, Wang JJ, Yang XH, Xiong Y, Wang NL, Friedman DS. Refractive Errors in a Rural Chinese Adult Population: The Handan Eye Study. Ophthalmology. 2009;116(11):2119-27.

8. Saw SM, Goh PP, Cheng A, Shankar A, Tan DTH, Ellwein LB. Ethnicity-specific prevalences of refractive errors vary in Asian children in neighbouring Malaysia and Singapore. Br J Ophthalmol. 2006; 90(10):1230-5.

9. Read SA, Collins MJ, Carney LG. A review of astigmatism and its possible genesis. Clin Exp Optom. 2007; 90(1):5-19.

10. Tong L, Saw SM, Carkeet A, Chan WY, Wu HM, Tan D. Prevalence rates and epidemiological risk factors for astigmatism in Singapore school children. Optom Vis Sci. 2002;79(9):606-13.

11. Maeda N, Klyce SD, Tano Y. Detection and Classification of Mild Irregular Astigmatism in Patients With Good Visual Acuity. Surv Ophthalmol. 1998;43(1):53-8.

12. Oshika T, Tomidokoro A, Maruo K, Tokunaga T, Miyata N. Quantitative evaluation of irregular astigmatism by Fourier series harmonic analysis of videokeratography data. Invest Ophthalmol Vis Sci. 1998;39(5):705-9.

13. Laíns I, Rosa AM, Guerra M, Tavares C, Lobo C, Silva MFL, Quadrado MJ, Murta JN. Irregular Astigmatism After Corneal Transplantation--Efficacy and Safety of Topography-Guided Treatment. Cornea. 2016;35(1):30-6.

14. Tanabe T, Tomidokoro A, Samejima T, Miyata K, Sato M, Kaji Y, Oshika T. Corneal regular and irregular astigmatism assessed by Fourier analysis of videokeratography data in normal and pathologic eyes. Ophthalmology. 2004;111:752-7.

15. Hayashi K, Kawahara S, Manabe S-i, Hirata A. Changes in Irregular Corneal Astigmatism With Age in Eyes With and Without Cataract Surgery. Invest Ophthalmol Vis Sci. 2015;56(13):7988-98.

16. Cox DJ, Banton T, Record S, Grabman JH, Hawkins RJ. Does correcting astigmatism with toric lenses improve driving performance? Optom Vis Sci. 2015;92(4):404-11.

17. Wills J, Gillett R, Eastwell E, Abraham R, Coffey K, Webber A, Wood J. Effect of simulated astigmatic refractive error on reading performance in the young. Optom Vis Sci. 2012;89(3):271-6.

18. Harle DE, Evans BJ. The correlation between migraine headache and refractive errors. Optom Vis Sci. 2006;83(2):82-7.

19. Gunes A, Demirci S, Tok L, Tok O, Koyuncuoglu H, Yurekli VA. Refractive Errors in Patients with Migraine Headache. Semin Ophthalmol. 2016;31(5):492-4.

20. Borderie VM, Laroche L. Measurement of irregular astigmatism using semimeridian data from videokeratographs. J Refract Surg. 1996;12(5):595-600.

21. Romero-Jimenez M, Santodomingo-Rubido J, Flores-Rodriguez P, Gonzalez-Meijome JM. Short-term corneal changes with gas-permeable contact lens wear in keratoconus subjects: a comparison of two fitting approaches. J Optom. 2015;8(1):48-55.

22. Shaheen MS, El-Kateb M, Hafez TA, Pinero DP, Khalifa MA. Wavefront-Guided Laser Treatment Using a High-Resolution Aberrometer to Measure Irregular Corneas: A Pilot Study. J Refract Surg. 2015;31(6):411-8.

23. Chen Z, Liu L, Pan C, Li X, Pan L, Lan W, Yang Z. Ocular residual and corneal astigmatism in a clinical population of high school students. PLoS One. 2018;13(4):e0194513.

24. F. Zernike, Beugungstheorie des schneidenver-fahrens und seiner verbesserten form, der phasenkontrastmethode, Physica1934; 7-12(1): 689-704.

25. Thibos LN, Applegate RA, Schwiegerling JT, Webb R; VSIA Standards Taskforce Members. Vision science and its applications.J Refract Surg. 2002;18(5):652-60.

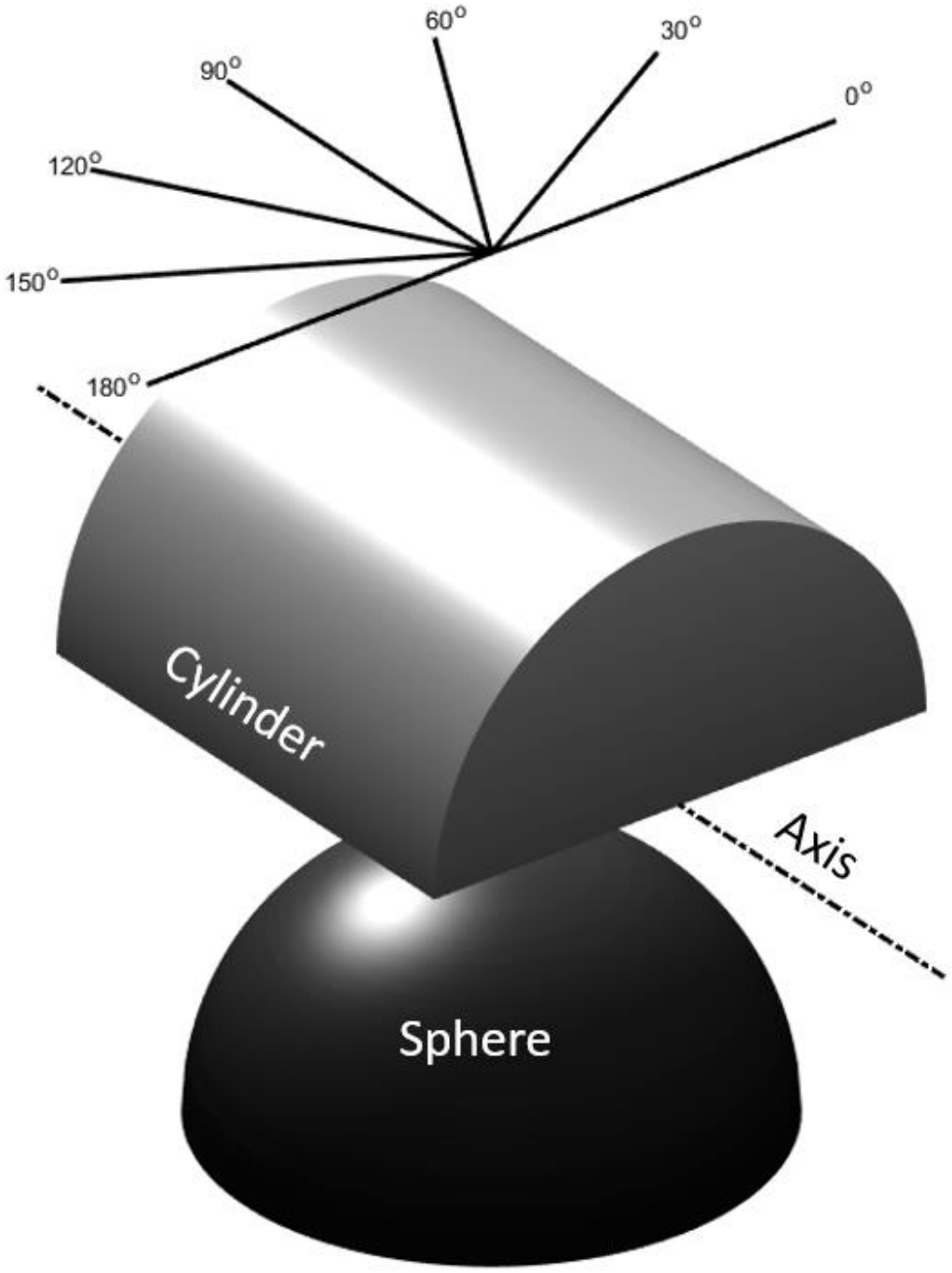

Figure 1: Forming a lens consists of spherical and cylindrical refractive bodies

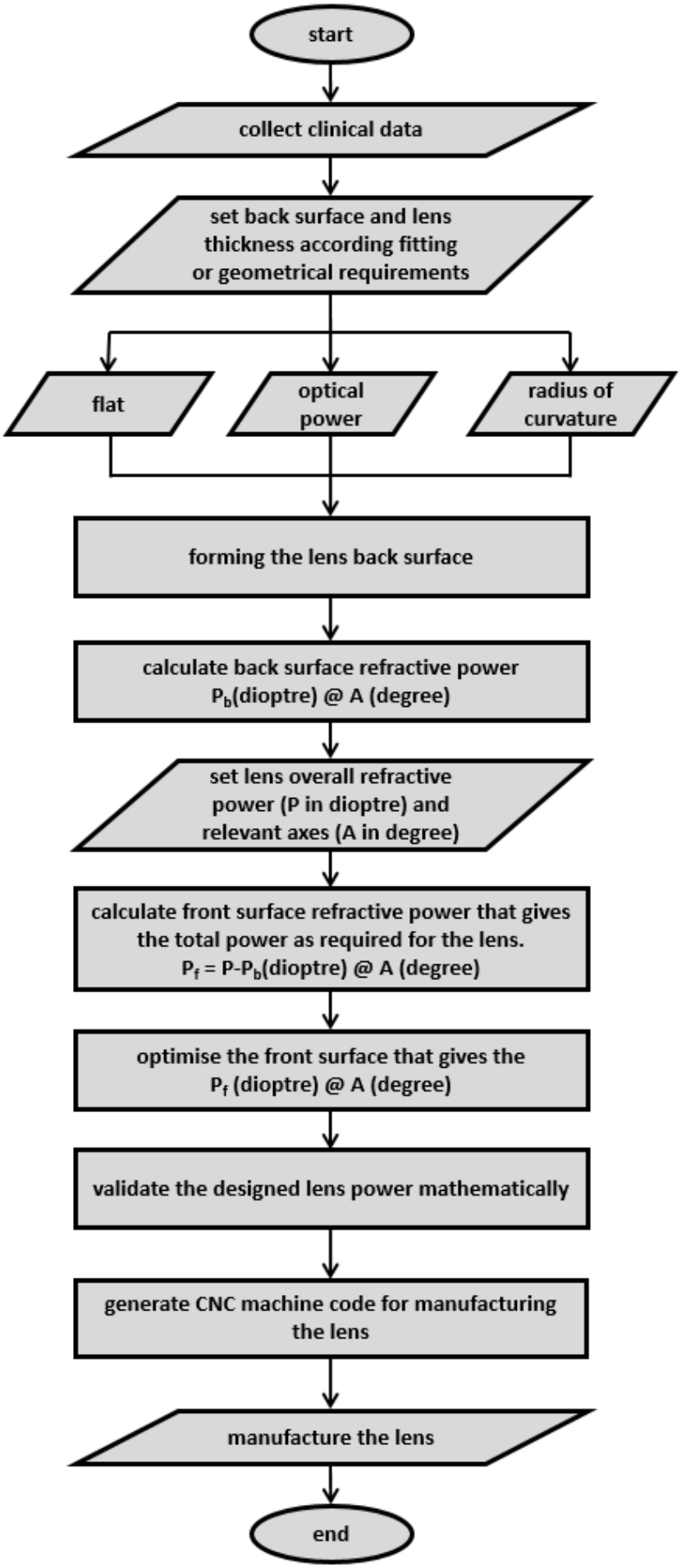
start
collect clinical data
set back surface and lens thickness according fitting or geometrical requirements
flat
optical power
radius of curvature
forming the lens back surface
calculate back surface refractive power P_b(dioptre) @ A (degree)
set lens overall refractive power (P in dioptre) and relevant axes (A in degree)
calculate front surface refractive power that gives the total power as required for the lens. $P_f = P\text{-}P_b$(dioptre) @ A (degree)
optimise the front surface that gives the P_f (dioptre) @ A (degree)
validate the designed lens power mathematically
generate CNC machine code for manufacturing the lens
manufacture the lens
end

Figure 2: Lens design flowchart

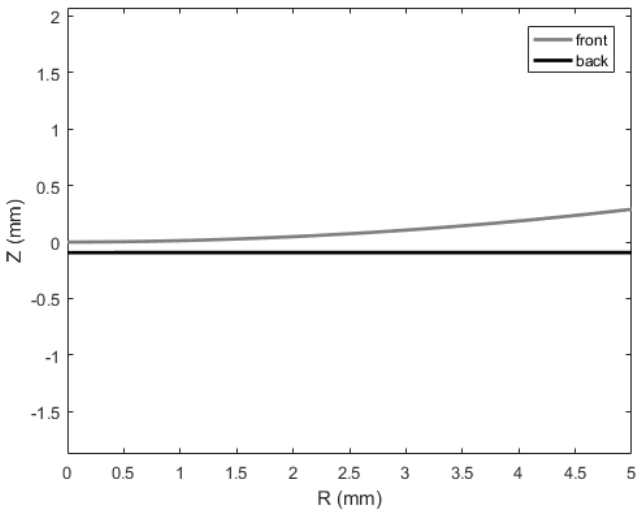

a

$P = -10, P_f = -10, P_b = 0$

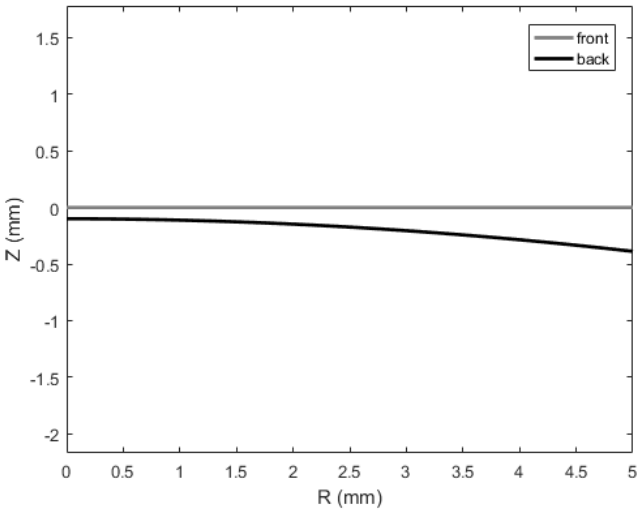

b

$P = -10, P_f = 0, P_b = -10$

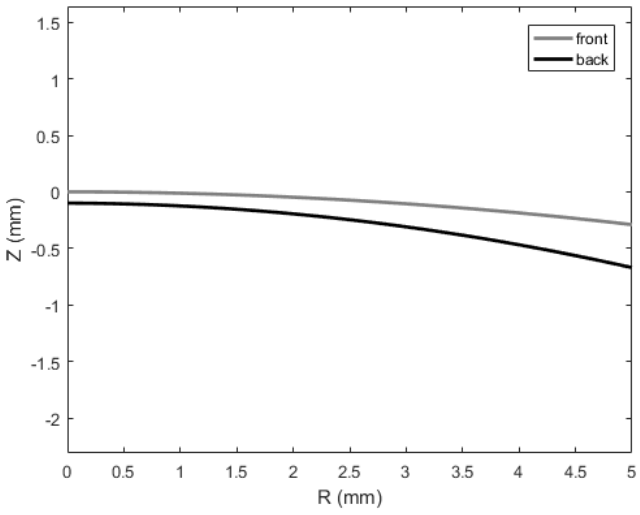

c

$P = -10, P_f = 10, P_b = -20$

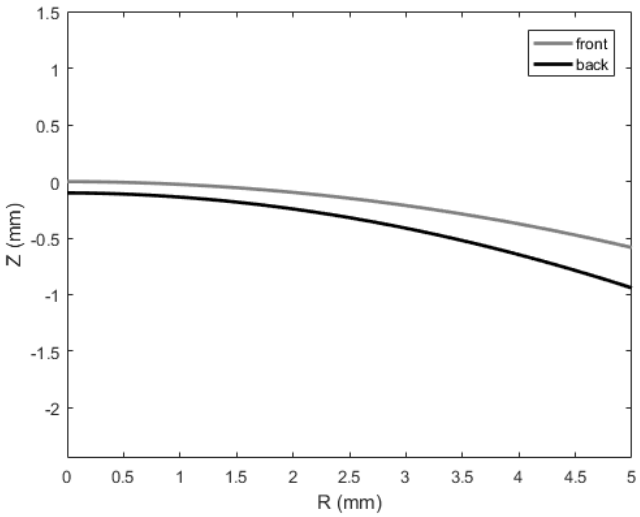

d

$P = -10, P_f = 20, P_b = -30$

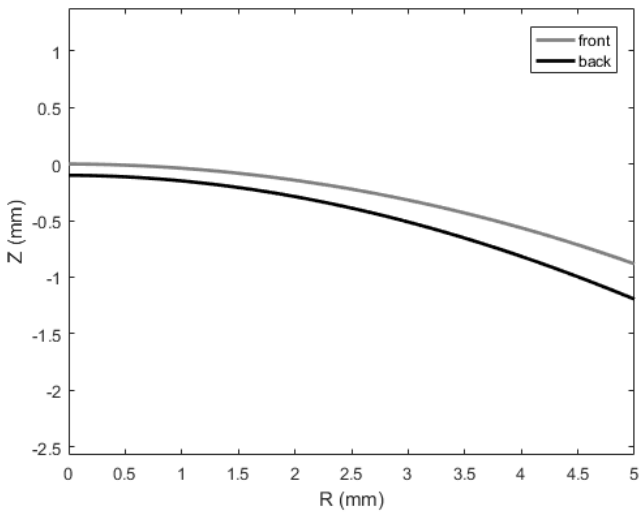

e

$P = -10, P_f = 30, P_b = -40$

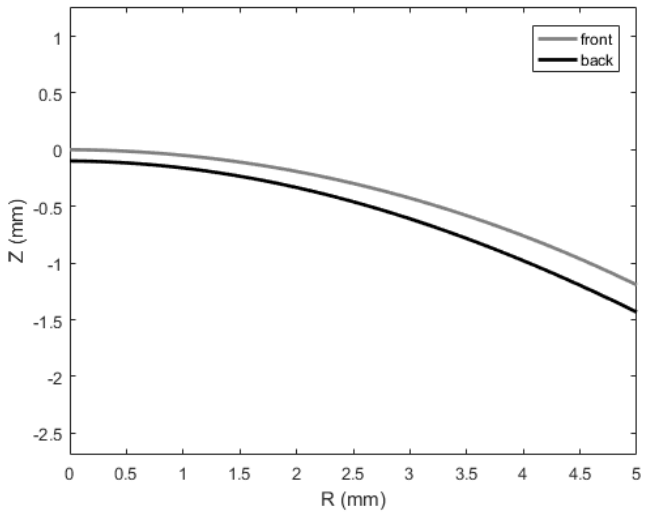

f

$P = -10, P_f = 40, P_b = -50$

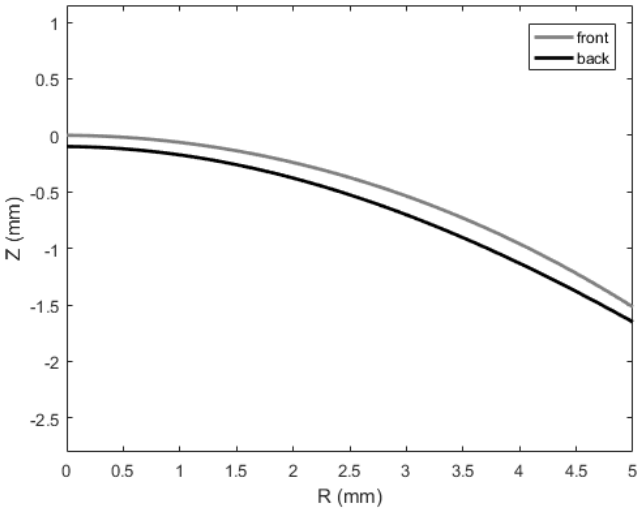

g

$P = -10, P_f = 50, P_b = -60$

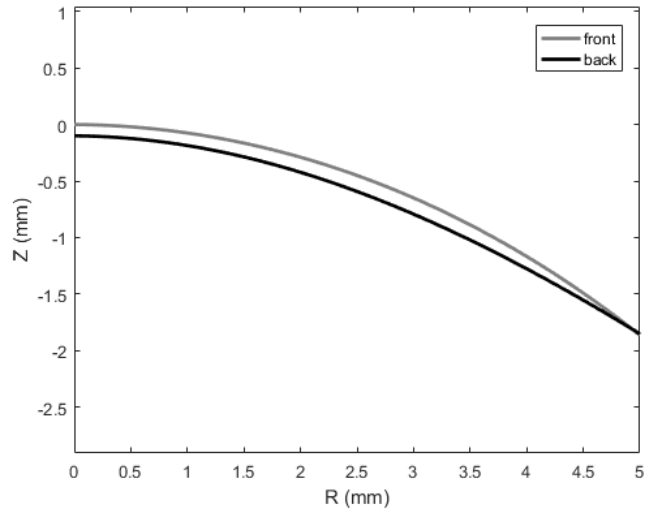

h

$P = -10, P_f = 60, P_b = -70$

Figure 3: Eight different designs for a lens with a power of -10 dioptre. The refractive index of the lens material was 1.44 and its central thickness was 0.25mm

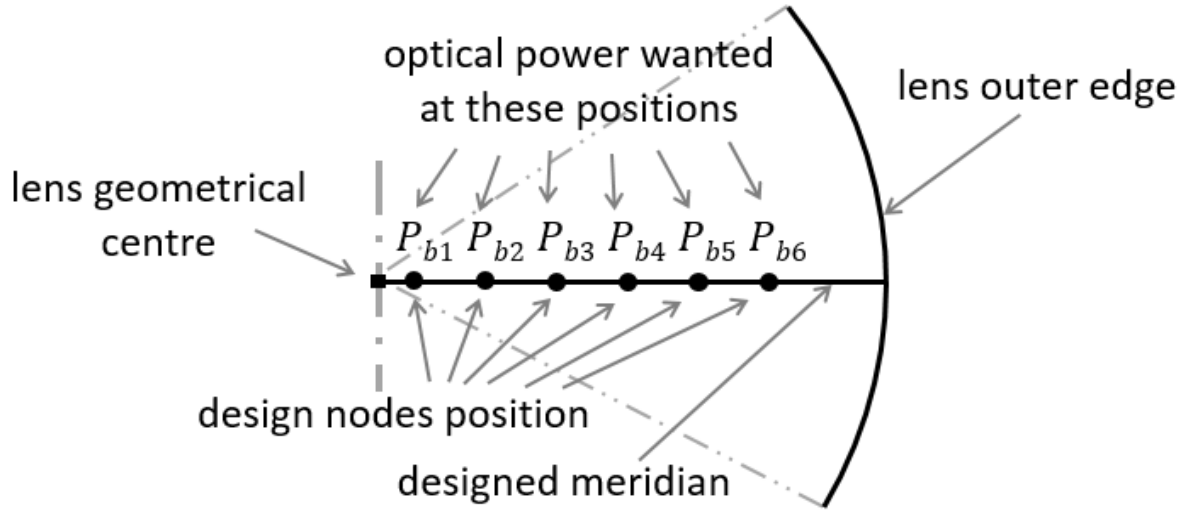

Figure 4: Designed meridian constructed from nodes

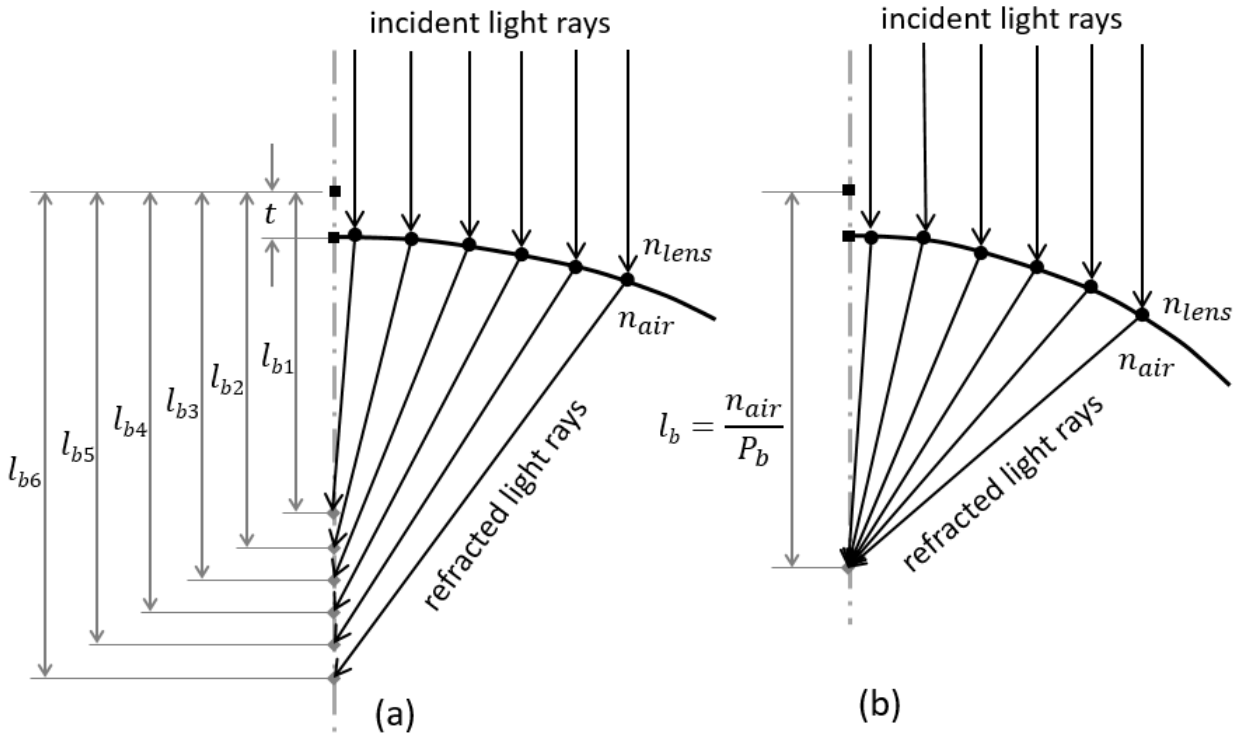

(A)

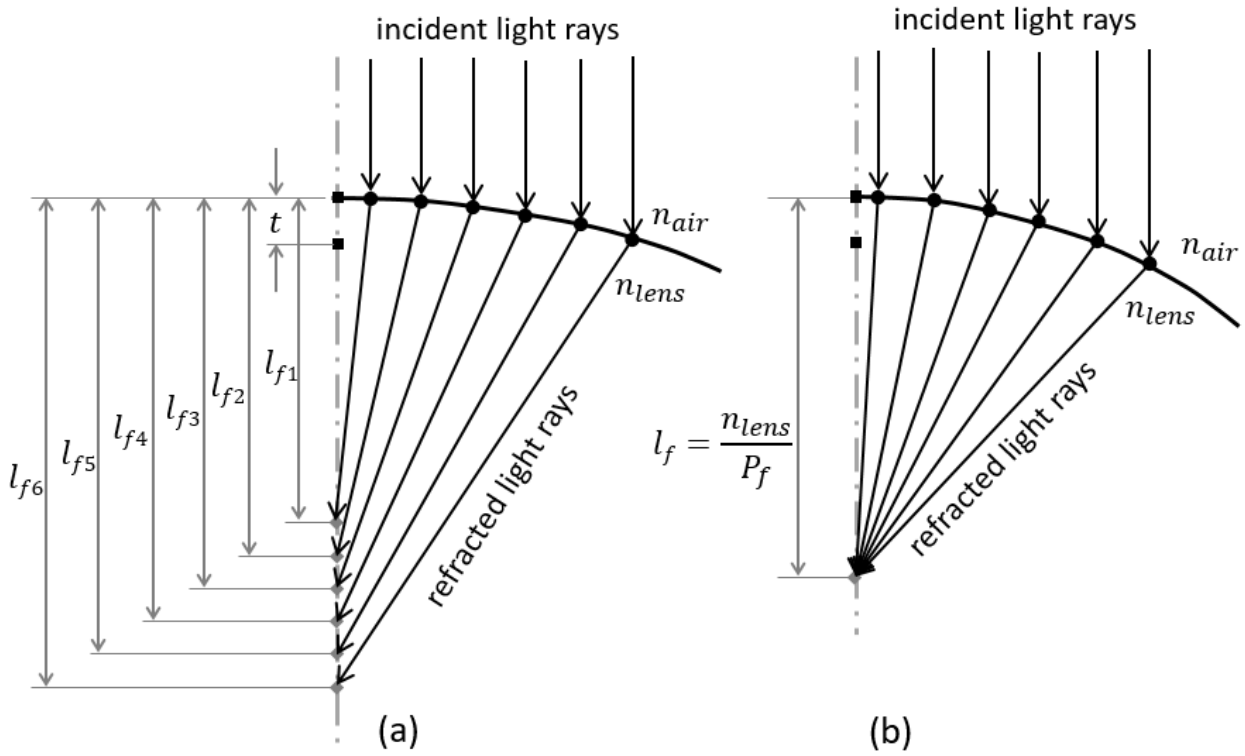

(B)

Figure 5: Lens surface design (A) Back surface design process, (B) Front surface design process

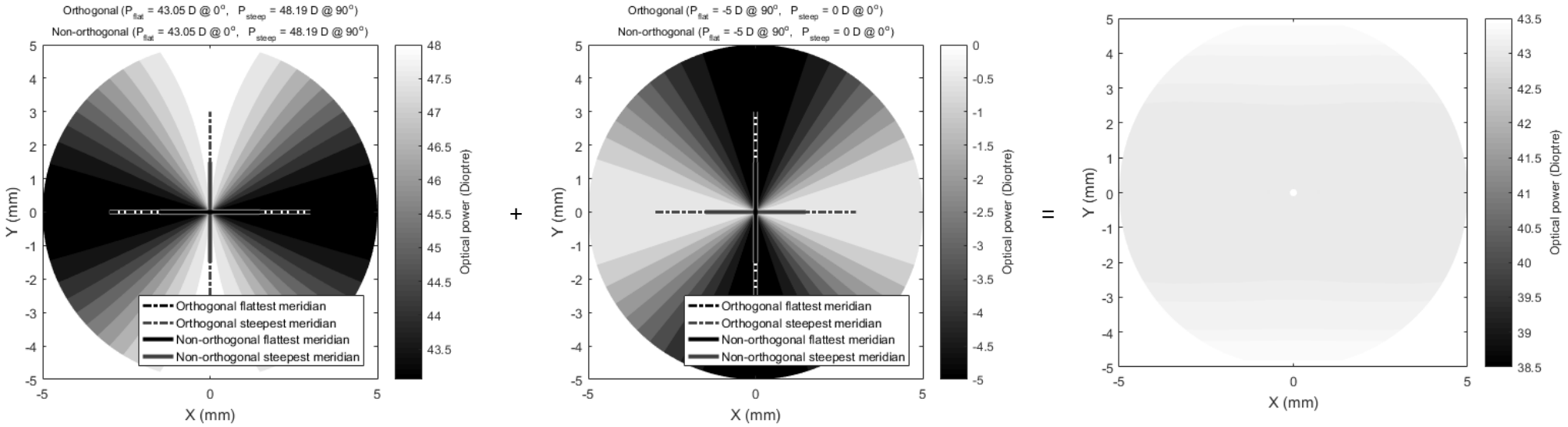

(a) Orthogonal astigmatic cornea (b) Orthogonal toric lens (c) Orthogonal correction

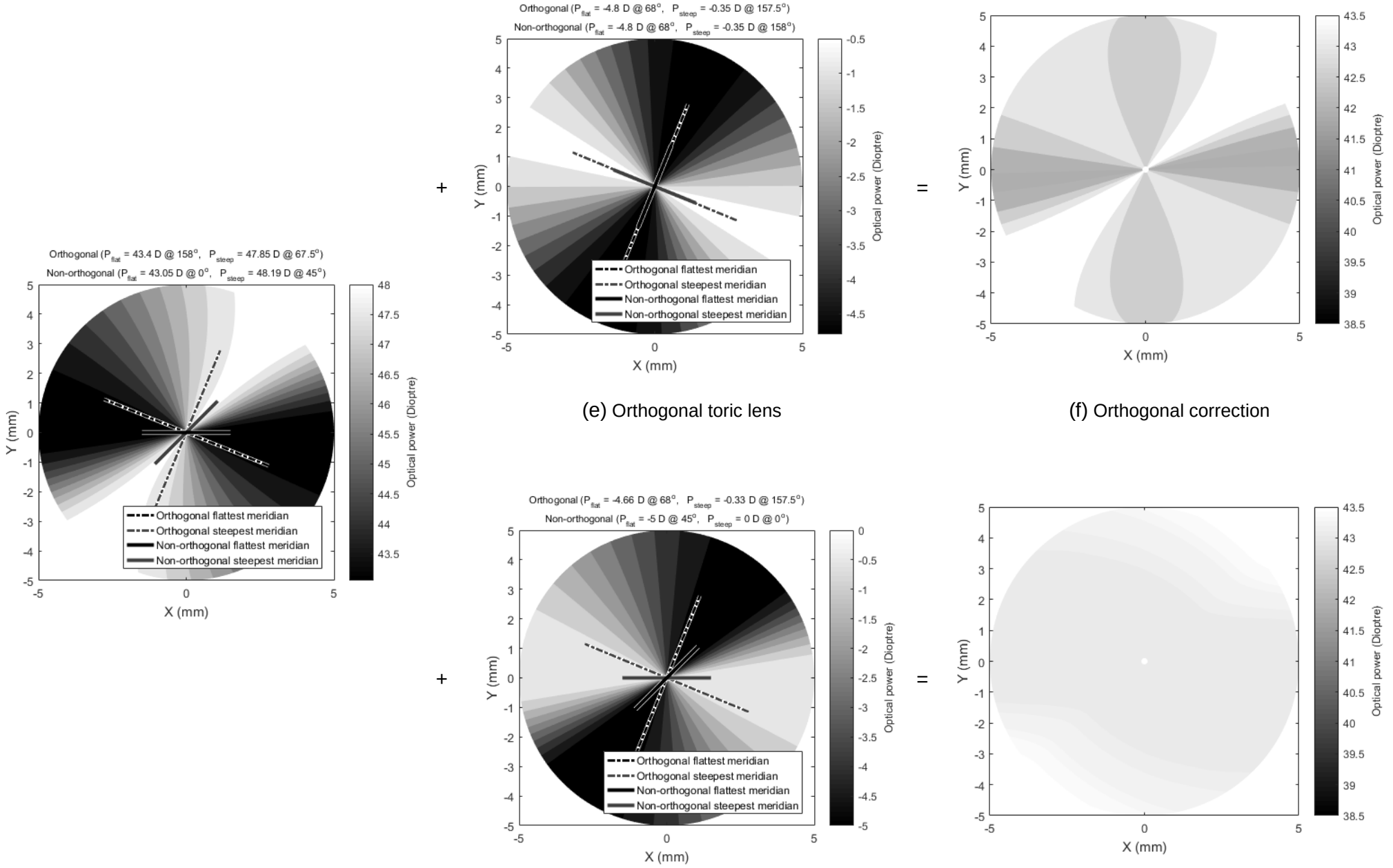

(d) Non-orthogonal astigmatic cornea

(e) Orthogonal toric lens

(f) Orthogonal correction

(g) Non-orthogonal lens

(h) Non-orthogonal correction

Figure 6: Theoretical justification of using a non-orthogonal lens design

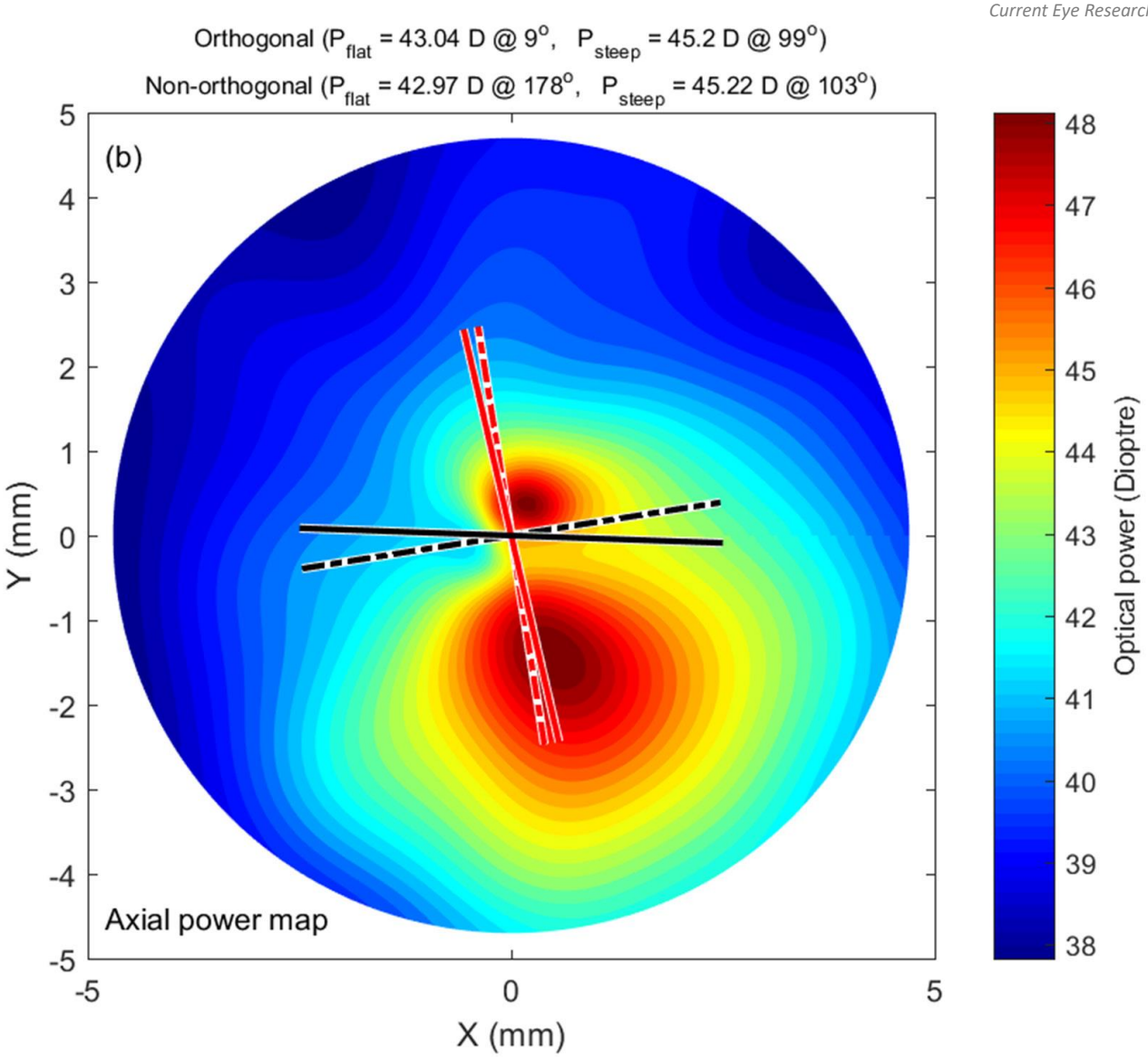

(A) Axial power map showing non-orthogonal axes at 75° (178°- 103°)

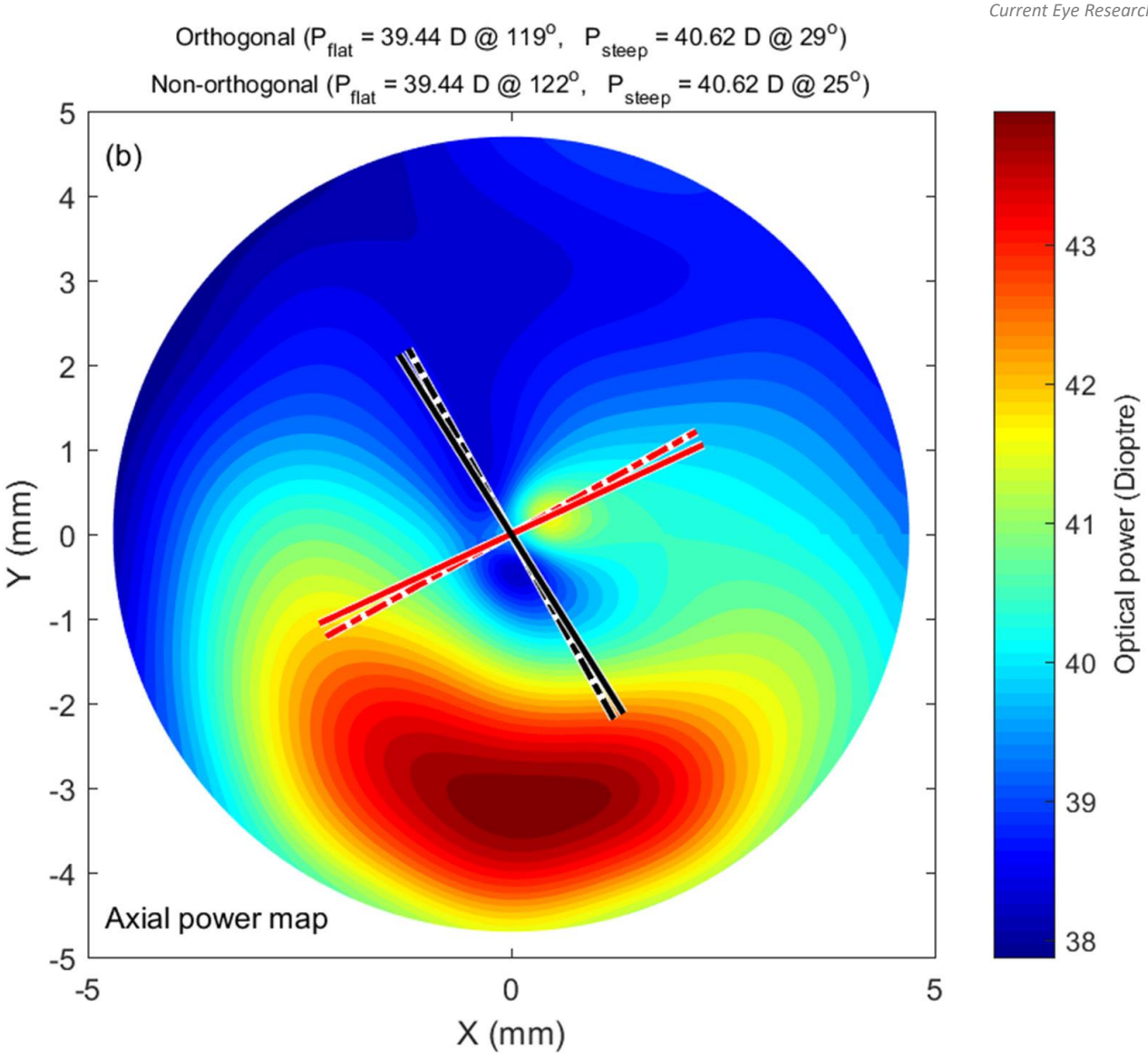

(B) Axial power map showing non-orthogonal axes at 97° (122°- 95°)

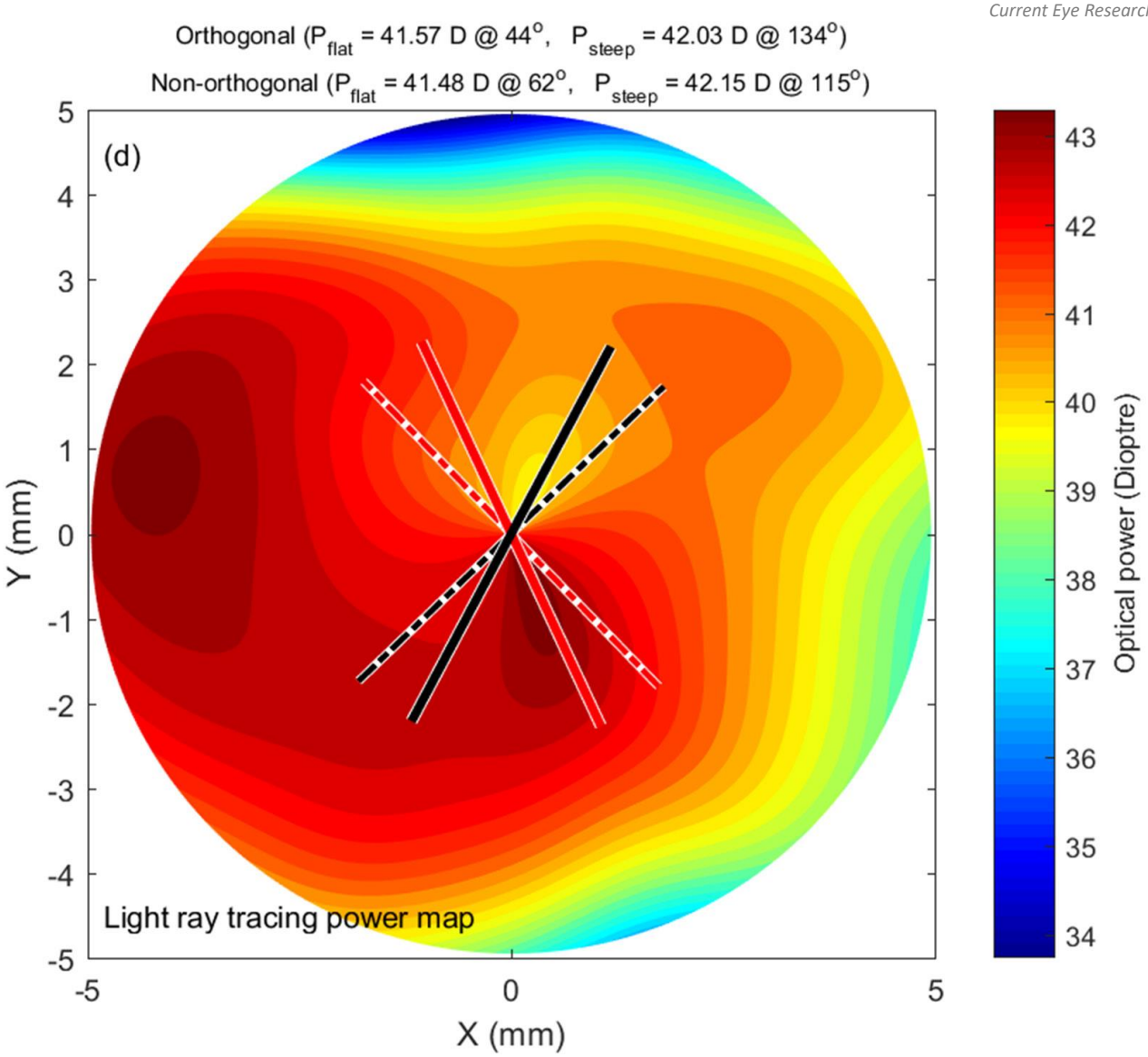

(C) Light Ray Tracing map showing non-orthogonal axes at 53° (115° - 62°)

Figure 7: Refractive power maps for participants